(26) Cochran, W.; Crick, F. H. C.; Vand, V. *Acta Crystallogr.* **1952**, *5*, 581.
(27) Yan, J. F.; Vanderkooi, G.; Scheraga, H. A. *J. Chem. Phys.* **1968**, *49*, 2713. The energy calculation for isolated poly(L-glutamates) in this paper indicates that this conformation of the side chain is the one of lowest energy.
(28) Fraser, R. D. B.; MacRae, T. P.; Miller, A. *Acta Crystallogr.* **1964**, *17*, 813.
(29) Watanabe, J.; Fukuda, Y.; Gehani, R.; Uematsu, I. *Macromolecules* **1984**, *17*, 1004.

Dynamic Light Scattering on Semidilute Solutions of High Molecular Weight Polystyrene in Ethyl Acetate

Wyn Brown

Institute of Physical Chemistry, University of Uppsala, S-751 21 Uppsala, Sweden.
Received May 6, 1985

ABSTRACT: Data obtained with quasi-elastic light scattering and gradient diffusion measurements on semidilute solutions in the $qR_g > 1$ range are presented for the polystyrene/ethyl acetate (marginal solvent) system. The time correlation function was analyzed by the method of cumulants and also fit by using one-, two-, and three-exponential expressions. Optimal fit was consistent with two exponents. The fast and slow components were both found to be q^2-dependent and also independent of molecular weight. It is concluded that two cooperative modes are required to describe a heterogeneous semidilute solution structure for polymers of high molecular weight. This agrees with the model of Brochard for poor solvent systems in the high-q region. The slower mode has a correlation length of the magnitude of the radius of the coil. Comparison with data in a good solvent (THF) and a Θ solvent (cyclopentane) show that D_f and D_s are strongly solvent-dependent as functions of concentration. This contrasts with the solvent-independent universal length recently demonstrated for the static parameter. The relative intensity contribution of D_f increased slowly with concentration as in the Θ system, in contrast to a rapid increase in a good solvent.

Introduction

There is currently a degree of confusion prevailing in the literature concerning the interrelationship between static and dynamic aspects of semidilute solution behavior and the way in which marginal solvents fit into the picture.

A feature that has been noted in quasi-elastic light scattering (QELS) studies is the systematic trend in the variance, μ_2/Γ^2, as measured by the cumulants method,[1] with increasing concentration.[2-6] The cumulants method, however, permits no further progress in understanding the possible causes that underly this behavior. Finite values of the line width in dilute solution reflect polydispersity, whereas in semidilute solutions a reasonable explanation for the relatively large variance is the presence of a small number of discrete exponentials describing complementary modes.[2,3] Such an assumption does not exclude the possibility of a more complex distribution of exponentials but is in line with current theory[7-10] for poor solvent systems and also finds support in elastic neutron and light scattering results[12] for polystyrene (PS) as semidilute concentrations in both good and poor solvents. If the possible validity of this view is conceded, a variety of approaches exist for analyzing the time correlation function and have been applied by various groups. Thus Chu and co-workers[2,3,11] used the histogram method to analyze $S(q,t)$ data for PS in poor solvent systems and interpreted the results in terms of two contributing modes of similar time scale. Other groups[5,13] have used CONTIN, a Fortran program introduced by Provencher.[14,15] The method of discrete multiexponentials has been used by others.[6,16-20] There will inevitably exist a measure of disagreement on the relative virtues of the various methods, and an objective appraisal of the particular advantages of the approaches is at present lacking. We use the method of discrete multiexponentials, which, although requiring an assumption of the number of participating relaxation processes, has particular relevance here. Recent reports described QELS measurements on the same polystyrene fractions at semidilute concentrations in both a good solvent (THF)[19] and in a Θ solvent (cyclopentane)[20] in the gel region. In the good solvent system the data were found to be consistent with the presence of fast and slow components differing in relaxation time by a factor of typically 3–5, whereas only a single gel mode was anticipated from theory.[7,8] A method of analysis having high resolution was thus essential. By the use of both computer-simulated experiments and measurements on mixtures of monodisperse fractions, it was established that the presently used method gives superior resolution when the relaxation times approach each other. It was suggested[19,20] that the modes separated, both of which are molecular weight independent, must reflect a fundamental heterogeneity of the semidilute solution structure. The slow mode was viewed in these papers as distinct from that which has been the subject of recent debate.[5,13,21-24] The latter is frequently orders of magnitude slower than the fast mode and may be separated experimentally by varying the sampling time. There is evidence[13,21,24] suggesting that this slow mode derives from the dynamics of clusters of chains.

Earlier reports[25-28] in which data interpretation was based on the assumption that the dynamic structure factor is a single exponential will need reappraisal if the gel mode is in fact a composite quantity in semidilute solutions. For example, the power law characterizing the concentration dependence will be strongly influenced by the change in the relative weighting between the modes over a given concentration interval.

The present paper has two aims: one is to further examine the nonuniform nature of semidilute solution structure, and the other is to elucidate the influence of solvent quality on the behavior of the transient gel.

Dynamic behavior in so-called "marginal" solvents, i.e., those in which there are only weak excluded-volume interactions, is still controversial. A QELS study[6] on PS of lower molecular weight, in solvents including ethyl acetate, established that the time correlation functions are strongly nonexponential and could be fit with a bimodal function. However, the interpretation to be placed on these com-

0024-9297/86/2219-1083$01.50/0

ponents in the framework of existing theoretical descriptions is unclear. The slower mode was interpreted there as a translational component. Schaefer et al.[27] used mean field theory to describe the binary interactions in such systems, and this approach led to predicted behavior that did not lie as might be anticipated intermediate between that postulated by scaling theory for good and Θ solvents. The earlier data[6] in contrast did suggest intermediate behavior. There is thus not only an element of discord on the model to be used for marginal solvent systems but also the possibility that this ambiguity is related to the method used in analyzing QELS data. The present paper describes QELS measurements on three high molecular weight PS fractions in ethyl acetate with the objective of clarifying the above issues. The results are supplemented with data from macroscopic gradient diffusion. Data for this system are subsequently compared with data for the same fractions in the good solvent[19] and Θ systems.[20]

Experimental Section

Polystyrene ($M = 3 \times 10^6$, $M_w/M_n = 1.06$; $M = 8 \times 10^6$, $M_w/M_n = 1.08$; $M = 15 \times 10^6$, $M_w/M_n = 1.30$) was obtained from Toya Soda Ltd., Japan. The ethyl acetate was spectroscopic grade from Merck, West Germany, and used without further purification except that it was dried over 3-Å molecular sieves.

Solutions. Sample and solvent were weighed into glass vials, and these were slowly rotated for 4 months at room temperature. The solutions were cooled to about −15 °C in an acetone/ice mixture while sealing the vials. It is important not to freeze the solutions since microcrystallites then form in the solution. The solutions were filtered extremely slowly in a closed-circuit filtration unit for usually two passes through a 3-μm Fluoropore filter. Such a procedure gave completely dust-free solutions as far as could be ascertained by observation of the scattering volume through a microscope and from signal stability. The solutions were then bled off into 10-mm-diameter, precision-bore NMR tubes. Dilutions were made by similarly treating solvent (0.2-μm filter) and adding to the weighed tubes. Higher concentrations were prepared by very slow evaporation of solvent from a known amount of the solutions in the light scattering tubes in a dust-free atmosphere. Degradation may potentially occur during solution preparation. Since, however, the semidilute solutions having bimodal correlation functions gave single-exponential curves at high dilution, this seems unlikely. In poor solvents and with high molecular weights there will be a very slow approach to equilibrium conditions. The measurements were thus repeated after 6 months from preparation of the solutions. Neither the D values nor their relative intensities changed significantly over this period, indicating that a stable arrangement of the entanglement structure exists.

Dynamic Light Scattering. All data were obtained in the homodyne mode with full photon-counting detection and a 128-channel Langley–Ford autocorrelator. Incident radiation at 488 nm was from a Coherent Super-Graphite 4-W argon ion laser containing a quartz etalon frequency stabilizer in the cavity to ensure single-mode operation to enhance the signal-to-noise ratio.

The quality of the data has been substantially improved over that of the earlier investigation[6] through use of an automatic data collection procedure. With the latter, approximately 60–80 runs, each of 1 s in length, are accumulated by using minimization of the total intensity and added together for each set of measurement parameters. Thus a comparison of the total intensity per second (I) of each run is made with the preceding run. If it lies within ±4% (2σ) it is accepted if higher the run is rejected. If outside this range and lower, all earlier runs are rejected and a new set of runs of accumulated relative to the new intensity standard until at least 60 runs falling within ±4% have been assembled.

This procedure has substantially eliminated any extraneous contributions from dust and gives data with a variance improved by at least an order of magnitude compared with manual operation of the correlator. The statistical base line (i.e., total pulses times the mean number of pulses per sampling time) was of the order of 2×10^7. Initially, each sum of runs accumulated as described above was analyzed with a three-term cumulants program to assess the quality. Only runs in which the statistical base line agreed closely with the value from the delayed channels were used and those with deviant intensity rejected. The general level of the data precision corresponded to a variance of 2×10^{-7} (standard deviation of the error 4×10^{-4}).

Data Analysis. The correlation function was treated interactively with the same microcomputer as that employed for data collection and reduction. The programs used were written in Forth for rapidity and compactness, and the microcomputer was fitted with an arithmetic processer for increased speed and accuracy. The time correlation function was treated as described in earlier papers[6,19,20] with a multiexponential routine based on an equally weighted nonlinear regression procedure with nonnegativity constraint according to the equation

$$g^{(2)}(\tau) - 1 = \beta[A_s \exp(-\bar{\Gamma}_s\tau) + A_f \exp(-\bar{\Gamma}_f\tau)]^2 \quad (1)$$

A_s and A_f refer to the relative intensity amplitudes, $\bar{\Gamma}_s$ and $\bar{\Gamma}_f$ are the corresponding relaxation rates, and β is an instrumental parameter, here approximately 0.65. Comparison of fits was made with equations of the form of eq 1 with one, two, or three exponential terms and with and without a base line term. The quality of the data fitting was estimated partly on the basis of the Q function

$$Q = 1 - \frac{\sum_{i=1}^{n-1} \epsilon_i\epsilon_{i+1}/(n-1)}{\sum_{i=1}^{n} \epsilon_1\epsilon_1/n} \quad (2)$$

If there is no grouping of residuals, ϵ, Q will approximate unity. The present system could be optimally fit with a four-parameter function without a base line term. In some cases, however, a base line correlation of some 1–2% gave a slightly lower value of χ^2, where χ^2 is the reduced sum of the squares of the residuals to the fit. The presence of a base line term in these instances did not, however, significantly change the amplitudes and relaxation rates. The necessity of including a base line term is apparently related to the solvent quality. Thus in the good solvent THF,[6,19] the base line term was negligible for values of the reduced concentration of up to $C/C^* = 200$. On the other hand, in the Θ solvent cyclopentane,[20] there was a significant amount of a base line term and this increased in weight with concentration. It appeared to derive from a q-independent structural relaxation. It is also noted here that the degree of nonexponentiality of the time correlation function changes progressively with solvent power. Thus, for example, with 8×10^6 PS at a concentration of 2% and at a scattering angle of 40°, the value of the normalized second cumulant, μ_2/Γ^2, is 0.22 (THF), 0.7 (ethyl acetate), and 1.02 (cyclopentane, 21 °C).

As pointed out in the Introduction, the bimodal fit used here is only the most simple of numerous alternatives that may be consistent with the information contained in the

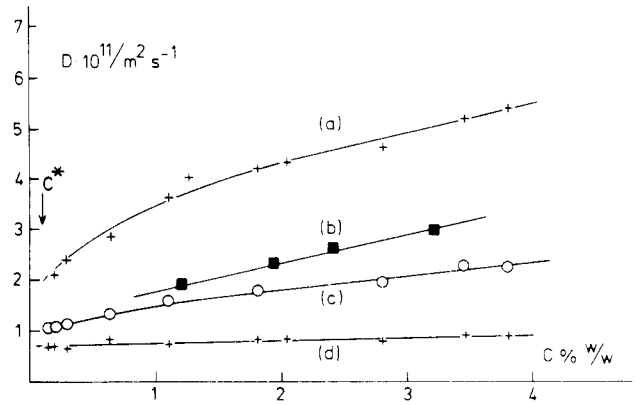

Figure 1. Concentration dependence of diffusion coefficients for semidilute solutions of PS ($M = 8 \times 10^6$) in ethyl acetate at 25 °C: (a) fast cooperative mode D_f; (b) $\bar{D}_{CGD}$, from gradient diffusion measurement (■); (c) D_{cum} from cumulant evaluation (○); (d) slow cooperative mode, D_s. D_f and D_s have been evaluated as the best slope from plots as illustrated in Figure 2 at each concentration. The 95% confidence interval falls within the size of the point in each case. $C^* = 0.08\%$.

correlation function. Alternative approaches to evaluating the contributions causing the nonexponentiality include analysis with programs such as CONTIN introduced by Provencher[14,15] and the SIMPLEX approach of Zimmermann et al.,[30] which require only the correlation function and the range of possible relaxation times. An extensive series of simulations has been made[6,29] to establish both the reliability and limitations of the present fitting procedures. Normally distributed pseudorandom numbers of a size typical of the residuals in a real run were added to "experiments" constructed with parameter values corresponding to the range of the actual runs. It was found that when the relaxation rates differ by at least a factor of 2 the minor component in, for example, a bimodal fit is well defined when contributing as little as 5% of the total scattering amplitude. Resolution of the two exponents, however, requires that they differ in relaxation rate by at least 30%. For the present data the relaxation rates of the two components differ by typically 3–5 μs (see, for example, Figure 1) which provides a congenial condition for their separation. Furthermore, the relative intensity contributions are well apportioned (see below). We thus have confidence in the results obtained when using eq 1 with the present data. As mentioned above, the presently used method gave better resolution than the other techniques in the cases studied and also better separation of mixtures of monodisperse fractions in dilute solution. There will inevitably exist possible ambiguity in the interpretation. For this reason the existence of static light scattering data that substantiate the presence of two modes[12] is important. As will be shown below, an interpretation in terms of two modes gives a consistent framework in several solvent systems and with different molecular weights and provides an insight into the dynamics that is not achieved with the cumulants approach.

Classical Gradient Diffusion measurements were made with a shearing-type cell[31] for free diffusion and a schlieren optical system. The half-width at the inflection point (ΔX) was measured in a microcomparator and $(\Delta X)^2$ plotted vs. time. The mutual diffusion coefficient was evaluated from the slope according to

$$(\Delta X)^2 = 2D_m t \quad (3)$$

The starting time correction was always zero within experimental errors; otherwise the experiment was rejected. D values were also calculated with the height–area method.

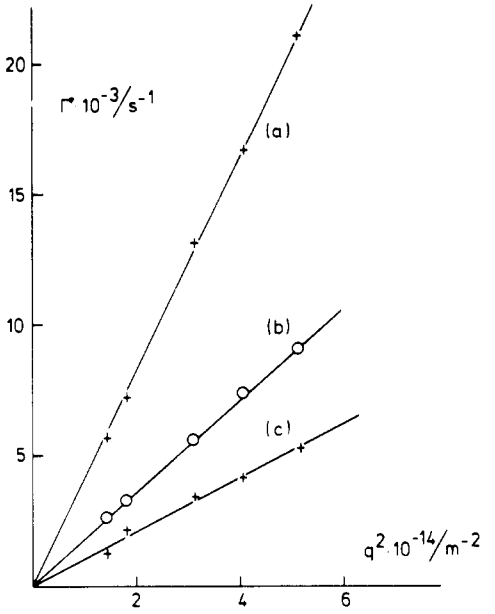

Figure 2. Relaxation rate, Γ, vs. square of the scattering vector, q^2, for data evaluation using bimodal analysis (eq 1). Results for a semidilute solution ($C = 1.47\%$ (w/w)) of PS ($M = 8 \times 10^6$) in ethyl acetate at 25 °C; (a) Γ_f is a fast cooperative mode; (c) Γ_s is a slow cooperative mode; (b) is for data evaluated with the cumulant method, $\bar{\Gamma}_{cum}$.

The two procedures gave values that were identical within experimental error. The boundary was always made between two solutions differing in concentration by about 1%, which was sufficient for accurate determination of boundary width. The diffusion coefficients then correspond to the average value, $\bar{C}$, across the boundary. It was established that in dilute solution the diffusion coefficients agreed well with values obtained from dynamic light scattering using cumulants evaluation.

Results

Dynamic light scattering measurements have been made on three fractions of polystyrene ($M = 3 \times 10^6$, 8×10^6, and 15×10^6) in ethyl acetate as a function of concentration and scattering angle. Most measurements have been made in the semidilute region up to a reduced concentration, $C/C^* = 50$ (see ref 44).

Figure 1 shows results of the analysis into discrete exponentials using eq 1 for the sample of $M = 8 \times 10^6$. Both fast and slow modes are interpreted as being diffusive motion on the basis of the linear relationships obtained between the relaxation rates, Γ, and the square of the scattering vector, q^2, as exemplified in Figure 2. Each pair of points corresponding to those on curves a and d in Figure 1 has been obtained from the slope at low q of plots as in Figure 2 at each concentration. The fast component (line a) is attributed to a gel mode (D_f)—the evidence for this interpretation has been presented in earlier papers.[19,20] D_f increases both in relaxation rate and relative intensity as concentration increases, particularly so in a good solvent[19] as anticipated for the pseudogel.[7,8] The values for the slower mode (D_s, line d) fall on a continuation of the line for the translational diffusion coefficient as evaluated in dilute solution from measurements at low angles where the condition $qR_g < 1$ is met. The time correlation function then closely approximates a single exponential.

The present approach in extracting information from the time correlation function differs from that of Munch et al.[26] and Schaefer et al.[27] for the PS/ethyl acetate system. They used a cumulant procedure[1] and evaluated only a single average diffusion coefficient from the time cor-

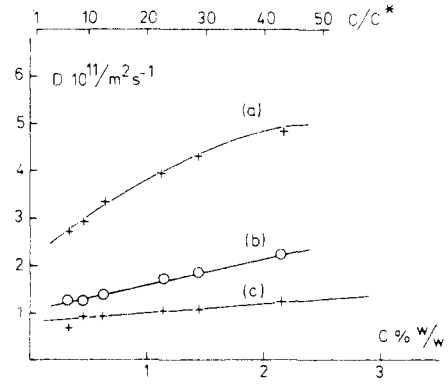

Figure 3. Data analogous to those in Figure 1 but here for $M = 15 \times 10^6$. Curves a and c are respectively for the fast cooperative mode and the slow cooperative mode using eq 1. Curve b is for cumulant evaluation of the data, $\bar{D}_{cum}$.

relation function even though it was recognized that they were strongly nonexponential. Discussions of the dynamics of the cooperative gel mode(s), however, must necessarily be based on the unadulterated component(s). The cumulant evaluation will only be meaningful if the distribution is known to be unimodal. The combined data[6,19,20] indicate that a uniform gel mode exists only as a hypothetical asymptotic limit, and in general (for very high molecular weights at least) one must take into account the component modes in the $S(q,t)$ data through some form of analysis of the correlation function. Under well-chosen experimental conditions, the gel mode can then be separated with acceptable precision.[19,20]

Figure 1 includes values of the diffusion coefficient obtained with the method of cumulants (curve c). These values will, for a bimodal distribution, correspond to the weighted average of the two modes (a and d). Also included are data obtained with the macroscopic gradient method (D_{CGD}); this gives an averaged quantity over the various modes contributing to the decay of the concentration gradient between two solutions.

Figure 3 shows data for the fraction with $M = 15 \times 10^6$. These agree closely with those in Figure 1. A fraction with $M = 3 \times 10^6$ was also examined and the overall agreement between the data will be shown in Figure 6 for the derived dynamic correlation length, ξ_D. Thus both fast and slow modes are molecular weight independent at $qR_g > 1$.

It may be observed that the present division into fast and slow components differs from that of Mathiez et al.[18]—their modes were widely separated and the intensity of the slow mode increased with concentration. In the present data, the modes cannot be separated by varying the sampling time, for example, and the relative intensity of the *fast* mode increases with concentration.

The relative contribution to the total intensity from the fast mode is illustrated as a function of concentration and angle and compared with similar data for the THF and cyclopentane (Θ system) in Figure 4. The comparatively small contribution in the poor solvents contrasts with that in THF. The relative amplitude changes only slowly with angle, the correlation function being distinctly bimodal even at the lowest measurement angle ($\theta = 30°$), for which $qR_g \simeq 0.8$. This aspect was discussed by Nishio and Wada,[16] who investigated the dynamics of polystyrene ($M = 10^7$) in another marginal solvent, 2-butanone. As the semidilute region is approached from the dilute region, a long tail becomes associated with the correlation function and a fast mode manifests itself at low values of q^2, where local motions cannot perturb the correlation function. The internal motions of a single coil in the dilute region have

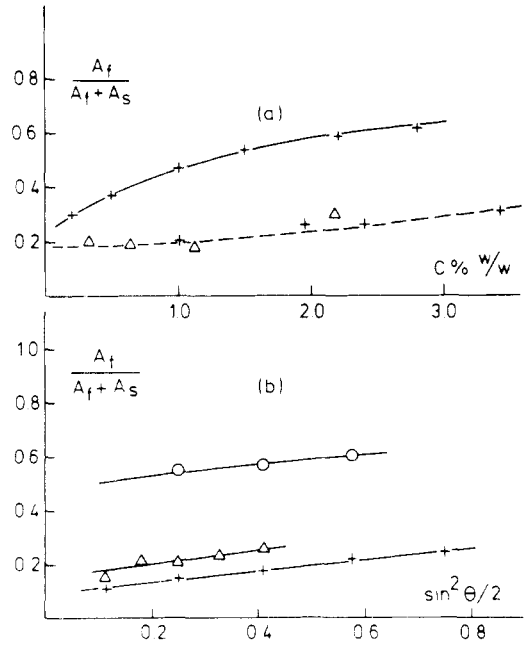

Figure 4. Relative intensity amplitudes, $A_f/(A_f + A_S)$ for the fast component (eq 1) for PS ($M = 8 \times 10^6$) as a function of (a) concentration, and (b) $\sin^2 \theta/2$ in different solvents (THF (○); ethyl acetate (△); cyclopentane, 21 °C (+). The data in (b) are all for a concentration of 1.3% (w/w). Data in THF are from ref 19 and in cyclopentane from ref 20.

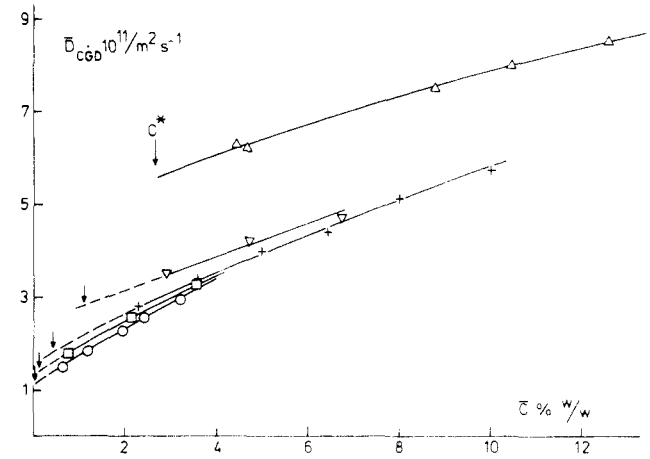

Figure 5. Classical gradient diffusion data for polystyrenes of different molecular weights in ethyl acetate at 25 °C. The vertical arrows indicate $C^* = 3M/4\pi R_g^3 N_A$.[44] $M = 9.3 \times 10^4$ (△); 2.8×10^5 (▽); 9.3×10^5 (+); 3×10^6 (□); 8×10^6 (○).

then become the cooperative motions of many overlapping coils above C^*. The gradient diffusion data are collected in Figure 5 with data for other molecular weights. Except for the lowest molecular weight fraction, the values are almost independent of M. This was also observed to be the case for the data in the good solvent. However, $\bar{D}_{CGD}$ was markedly dependent on M in the Θ system,[20] which is in accord with expectations since the gradient method will reflect also motions occurring on a time scale greater than the disentanglement time.

Discussion

Bimodal Separation. The two modes presently evaluated cannot be separated experimentally by using different sampling times. However, tests of the routine described in Data Analysis give confidence in the potential of the program used to separate components that are considerably closer in relaxation time than is the case for

the modes determined here. This conclusion was further strengthened by the analysis of mixtures of monodisperse fractions of different molecular weight. There will always exist a degree of ambiguity in the choice between alternative distributions that may have a similar statistical confidence measure using such parameters as the Q function and the χ^2 minimum. For this reason it is invaluable to have some independent evidence that the model used is well-chosen. The validity of the analysis made here thus rests on two features: 1. the demonstrated ability of the program to resolve bimodal simulations and synthetic mixtures; 2. the assumption that (at least in poor solvents) a two-exponential model is a reasonable expectation on theoretical grounds[10] (this is also found to be the simplest model that is consistent with the data). The present interpretation finds support in the elastic light and neutron scattering data of Koberstein et al.[12] The latter show that in both good and poor solvents the semidilute solutions examined are heterogeneous in structure, with a slow component having a correlation length of the magnitude of the radius of the coil. The implication of this is still unclear. At concentrations close to C^* it seems plausible to expect the presence of a translational component, but this becomes more unlikely at higher concentrations. It appears that the interpenetration is only partial and the network still reflects much of the original coil structure. This is essentially the model of Brochard[9,10] for poor solvents in which, due to self-entanglement effects, a high-frequency gel mode accompanies a slow osmotic mode in the high-q region where these are simultaneously probed.

The presently determined multiexponential behavior cannot be attributed to the presence of dust, although this is a source of considerable difficulty in investigations of more concentrated systems. The systematic trends in the data for all three solvents with the different molecular weights over a broad range of concentration provide evidence that such a trivial explanation is not valid here. The increase in the relative intensity of the fast mode with increasing concentration in all three solvents is also inconsistent with such an explanation, since the slow mode would then be the one to increase and also be expected to have a much lower relaxation rate than observed.

Interference from local modes must always be considered with measurements in the $qR_g > 1$ region and would also give rise to nonexponential correlation functions. The absence of significant angular dependence of the (Γ/q^2) ratio (see, for example, Figure 2) is support for rejecting this alternative, even though minor contamination is possible and may influence the value of the slope. The measurements have been made in a q region where (Γ_{cum}/q^2) is strictly angle-independent.

It is not suggested that a degree of coupling does not exist between the modes or that complete separation between them has been achieved. It has been found, however, that a bimodal model provides a consistent interpretation and that it is necessary in this or an analogous way to take into account the systematic and progressive change in the variance. The term "slow mode" may lead to some confusion, since some groups[5,21-24,28] describe a slow relaxation that is several orders of magnitude lower than the fast component. Such decays are featured with lower molecular weights at high concentrations in the $qR_g < 1$ region and also in Θ systems.[23] They are possibly due to the reptative motions of clusters of chains since the molecular weight and concentration dependences are close[21-24] to the values predicted for self-diffusion,[7,8] although the values of D are at least an order of magnitude lower.

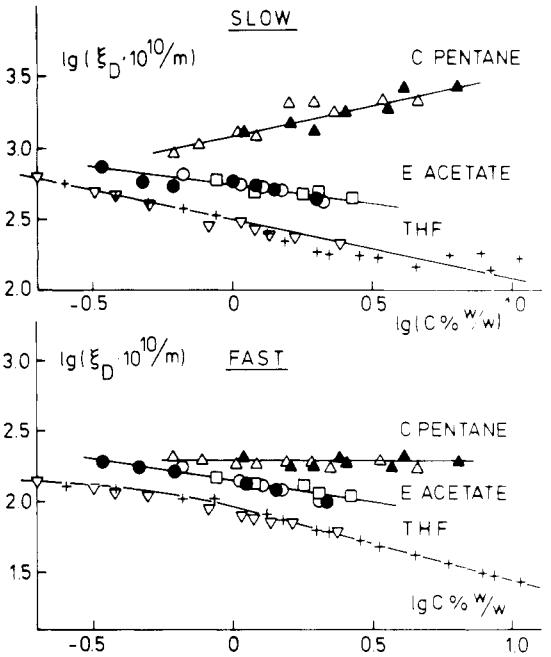

Figure 6. The dynamic correlation length, ξ_D, evaluated from the fast and slow modes obtained with eq 1 as a function of concentration in a log–log plot. Data are given in three solvents as shown and the following molecular weights: cyclopentane $M = 8 \times 10^6$ (△), 15×10^6 (▲); ethyl acetate 8×10^6 (○), 15×10^6 (●), 3×10^6 (□); THF 8×10^6 (+), 15×10^6 (▽); see Table I for slopes.

Solvent Dependence of Diffusion. Figure 6 shows the concentration dependence of the dynamic correlation length, ξ_D, where

$$\xi_D = kT/6\pi\eta_0 D \tag{4}$$

with $D = (\Gamma/q^2)_{q\to 0}$, k is Boltzmann's constant, and η_0 is the solvent viscosity. The data in Figure 6 have been obtained from the diffusion coefficients corresponding to the fast and slow modes, evaluated as described in Data Analysis, in three solvents and for two molecular weights ($M = 15 \times 10^6$ and 8×10^6). The data for the slower mode in THF (good solvent) scatter considerably due to the low-intensity contribution at high concentrations. It has been shown in previous communications[19,20] that in both THF and cyclopentane (Θ solvent) two diffusional modes are present in each and have relaxational rates differing by less than an order of magnitude. (The insert to Figure 8 shows an analogous plot for the cumulants-evaluated data.)

Figure 6 shows that the fast and slow modes are both molecular weight independent within experimental uncertainty and therefore are interpreted as of cooperative nature, describing the heterogeneity of the transient gel. The consistency of the data accumulated in Figure 6 for the two high molecular weight fractions over a broad range of concentration in the semidilute region establish that their dynamics are considerably more complex than hitherto recognized.

Figure 7 compares the data obtained at $qR_g > 1$ with those at $qR_g < 1$ for lower molecular weights.[6] In the latter case, use of eq 1 led to resolution into molecular weight dependent and molecular weight independent quantities. For concentrations not too far above C^*, this result is anticipated since both a translational mode and the gel mode are conceivably represented in the time correlation function. This finding also provides indirect support for the bimodal model. However, at $qR_g > 1$, it will not be possible to probe a translational component for large coils.

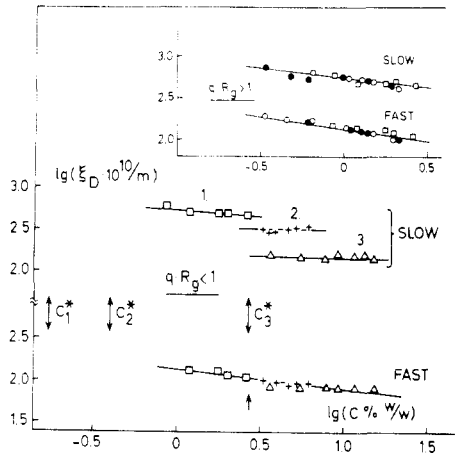

Figure 7. Log–log plot of ξ_D vs. concentration for data obtained at $qR_g < 1$ for fast and slow modes evaluated with eq 1 and 4. ($M = 3 \times 10^6$ (□), 9.3×10^5 (+), 9.3×10^4 (△). The insert shows an analogous plot for $qR_g > 1$ ($M = 15 \times 10^6$ (●), 8×10^6 (○), 3×10^6 (□)).

Table I
Solvent Dependence of the Exponent[a] in $\xi_D \sim C^\gamma$ (eq 4) from QELS Measurements

solvent	cumulants data	fast mode	slow mode	predicted gel mode exponent
THF	−0.67	−0.57	−0.44	−0.75[b]
ethyl acetate	−0.43	−0.33	−0.22	−0.75[b] (−0.50)[c]
cyclopentane (Θ)	−0.06	0	+0.45	0[d]

[a] All exponents refer to data corrected to the solvent reference frame[35] using the factor $(1 - \phi_P)$, where ϕ_P is the volume fraction polymer. [b] References 7 and 8. [c] Reference 27. [d] References 9 and 10.

Instead one has access to both (cooperative) hydrodynamic and gel relaxations as visualized by Brochard for semidilute Θ solutions.

The value of the exponent in $\xi_D \sim C^\gamma$ is one of the main indices used to assess the measure of agreement between theory and experiment. The presence of several modes complicates the picture considerably and may also be the cause of the scatter in the literature values of exponents. Error (or at least ambiguity) will attend the exponent when either a cumulants fit or a single-exponential approximation is used to evaluate the data in such cases. This problem also arises with use of the gradient technique, which gives an average D value.[32] Since the relative weighting between the modes will change, and perhaps strongly as a function of concentration, the slower mode will dominate close to C^* and the faster at $C \gg C^*$. Thus the exponent for the cumulant data, for example, will be inordinately high compared to the values for the individual modes (compare the exponents collected in Table I). Table I compares the exponents in $\xi_D \sim C^\gamma$ for the various systems, obtained from plots as in Figure 6. The values refer to data corrected to a frame of reference relative to the solvent velocity[33] using the factor $(1 - \phi_p)$ where ϕ_p is the volume fraction polymer. The data obtained with the cumulants evaluation are depicted in the insert to Figure 8. In THF the slope for the *fast* mode is −0.57, a value considerably lower than that expected from scaling theory.[7,8] The exponent for the *slower* mode is −0.44. In the Θ solvent cyclopentane, the measurements were made in the high-q region so that the gel mode is probed rather than the hydrodynamic mode (low-q region). Thus when $q \geq q_g$, (see ref 10) the exponent for the gel mode is predicted to be zero, contrasting with a slope of unity for the hydrodynamic mode. In cyclopentane the faster mode is found to be concentration-independent, in agreement with theory, whereas the slower mode exhibits a diffusion coefficient that decreases with increasing concentration. Ethyl acetate adopts an intermediate position, both as regards the value of the correlation length at a given concentration and the slopes for both fast and slow modes.

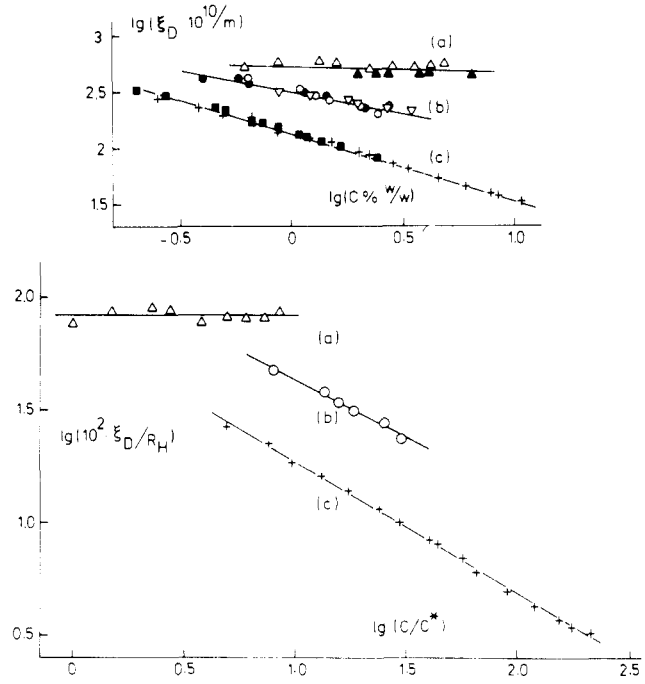

Figure 8. The reduced length (ξ_D/R_H) as a function of the reduced concentration (C/C^*) for $M = 8 \times 10^6$ in (a) cyclopentane, (Θ solvent), (b) ethyl acetate, and (c) THF. $\bar{D}_{cum}$ is used to evaluate ξ_D. The insert shows ξ_D as a function of concentration in the three solvents in a log–log plot. The filled points are for $M = 15 \times 10^6$. The points for $M = 8 \times 10^6$ are as shown in the main figure. Data for $M = 3 \times 10^6$ (▽) in ethyl acetate are included; see Table I for slopes.

Schaefer and Han[34] suggest that an exponent close to unity (which they refer to as Θ-like behavior) may be observed in good and marginal solvents at high concentrations (i.e., $\phi_p > 0.1$). With the present systems, PS/THF and PS/EA, no support is found for an increase in the exponent at the highest range of concentration in the semidilute region, even when the concentration extends up to 11% (w/w) for PS 8×10^6. It would appear that a common power law extends over the whole semidilute region, and no evidence is found for "transitions" to other exponents, as suggested by Schaefer and Han.[34] In point of fact, the divergent concentration regions they graph characterize different molecular weight samples; the support for transitions is thus much less convincing than if the data had been for a single fraction covering the whole span of concentrations.

It should be pointed out that the lower esters of acetic acid are unusual in that their solutions of polystyrene display both upper and lower critical solution points.[35] For ethyl acetate the corresponding Θ temperatures are Θ = −44 and +139 °C, both of which are, in principle accessible. The temperature/concentration diagram given by Schaefer et al.[27,34] for the PS/ethyl acetate system is thus misleading in its apparent simplicity. At intermediate temperatures (~25 °C) ethyl acetate is in fact a fairly good solvent. From intrinsic viscosity measurements we estimate that R_g is 0.85 times the value in the good solvent THF, contrasting with the suggestion[34] that ethyl acetate is close

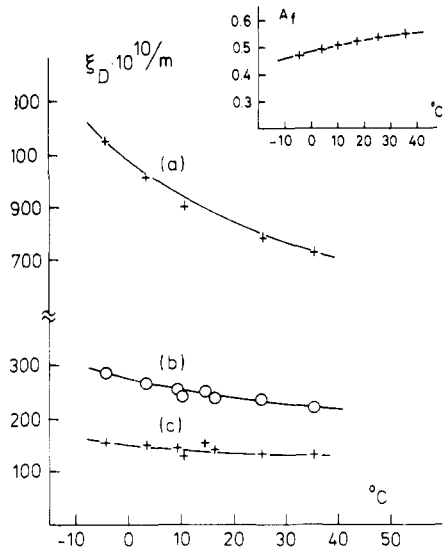

Figure 9. Dependence of the dynamic correlation length, ξ_D, on temperature. (a) and (c) are the slow and fast cooperative modes evaluated with eq 1; (b) is the evaluation with the cumulants $\bar{D}$ values. The exponents obtained from log–log plots are (a) −0.1, (b) −0.05, and (c) −0.04. The data are for $M = 3 \times 10^6$ in ethyl acetate at $C = 4.2\%$ (w/w). The insert shows the variation of the intensity contribution from the fast mode as a function of temperature.

to a Θ solvent (0.44 times the value of R_g in THF).

Scaling theory[7,8] predicts a universal relationship between the reduced correlation length (ξ/R_g) and the reduced concentration (C/C^*). Amirzadeh and McDonnell[37] and Wiltzius et al.[36] have shown that the static length scale, ξ, exhibits universal behavior for sufficiently large molecular weights. The latter used a log plot of the reduced length (ξ/R_g) vs. X, where X is a variable directly proportional to C/C^*. Figure 8 depicts an analogous plot for the dynamic correlation length, ξ_D, in which the hydrodynamic radius, R_H, has been used instead of R_g, where $R_H = \xi_D$ ($c \to 0$), for semidilute concentrations of PS $M = 8 \times 10^6$ in three solvents. In evaluating ξ_D, ($\Gamma_1 q^2$) has been employed, where Γ_1 refers to the initial decay rate, since it yields a length parameter most readily compared with the time-averaged quantity used by Wiltzius et al.[36] If the static quantity exhibits universal behavior in such a plot, then it may be concluded that the dynamic and static quantities have very different concentration dependences. That ξ and ξ_D are not proportional was shown by Adam and Delsanti.[38] In a subsequent communication, Wiltzius et al.[39] show that for solutions of low concentration in which the dependence of D_c on C is still linear, (ξ_D/R_H) is a universal function of kC, with k given by $D_C = D_0$ (1 + kC). We note here that the predicted identity of the static and dynamic correlation lengths has recently been called into question on theoretical grounds.[40] Furthermore, self-diffusion data[41] do not support the concept of a universal length scale. The insert to Figure 8 shows a log–log diagram of the dynamic correlation length vs. concentration, where $\bar{D}_{cum}$ has been used to derive the ξ_D values. The slope for the data in THF is −0.67, independent of molecular weight, after correction to the solvent frame, and this may be compared to the value of −0.43 in ethyl acetate (see Table I). The value of −0.67 in a good solvent has received support in the literature, but notably by groups[25,43] who assume a single-exponential decay process.

Measurements have been made on all three fractions over the range of temperature −10 to +36 °C. These measurements were made by cycling the temperature in both directions. Particular care was needed to ensure solution homogeneity on change in temperature, the mixing being very slow with concentrated solutions. Typical data at semidilute concentrations are shown in Figure 9. The dynamic correlation length decreases with increasing temperature—very slightly in the case of the fast mode and strongly for the slow mode. The latter behavior is possibly reasonable in light of the postulated partial interpenetration of coils as described above, since "overlapping" portions would be most sensitive to changes in interaction parameters. In any event, a more pronounced increase in the correlation length is anticipated as the Θ point at −44 °C is approached. Similar measurements on the Θ system PS/cyclopentane[20] have demonstrated this. The insert to the figure shows that the relative intensity amplitude is also relatively insensitive to temperature change, in contrast to the situation in systems close to the Θ point.

Conclusions

In common with good solvent and Θ systems, the marginal solvent system polystyrene/ethyl acetate is characterized by nonexponential time correlation functions throughout the semidilute region in the range accessible to QELS measurement. In the three solvents differing greatly in solvent power and with high molecular weights, two cooperative modes are substantiated. They have similar time scales (the relaxation rates differ by typically 3–5) and this feature complicates their separation. With existing routines, this may be achieved as has been demonstrated by Chu and co-workers[2,3,11] using the histogram method and by this and preceding papers[6,19,20] with the application of bimodal programs. These data, taken together, establish the hitherto inadequately recognized complexity of the dynamic structure factor for very high molecular weights in semidilute solution. The model of essentially noninterpenetrating coils has been used by Brochard[10] to describe the behavior of semidilute Θ solutions. It would appear that this view has validity even in the description of good solvent systems. This divergence from a single characteristic length for describing the structure of semidilute solutions constitutes a serious problem in light of scaling theory,[7,8] which rests on this supposition.

With lower molecular weights in good solvents, a uniform gel mode appears as the dominant feature above C^*. However, other complications may be met with, for example, the presence of a very slow mode at high concentrations ($\phi_P > 0.1$), which is apparently related to the motions of clusters of chains within the entanglement network.[6] In marginal solvents, intermediate molecular weight polymers yield a mixture of fast and slow modes above C^*, where the latter is attributable to translational motions. Thus the straightforward experimental isolation of a uniform gel mode would seem to represent an exceptional situation.

The weight of evidence serves to support the thesis that marginal solvents have no unique features differentiating them from the behavior expected in the trend from good to Θ solvent. Their dynamics are of intermediate character.

Registry No. PS, 9003-53-6; $H_3CCO_2CH_2CH_3$, 141-78-6.

References and Notes

(1) Koppel, D. E. *J. Chem. Phys.* **1972**, *57*, 4814.
(2) Nose, I.; Chu, B. *Macromolecules* **1979**, *12*, 590,599.
(3) Chu, B.; Nose, I. *Macromolecules* **1980**, *13*, 122.
(4) Yu, T. L.; Reihanian, H.; Jamieson, A. M. *Macromolecules* **1980**, *13*, 1590.
(5) Selser, J. C. *J. Chem. Phys.* **1983**, *79* (2), 1044.
(6) Brown, W.; Johnsen, R. M. *Macromolecules* **1985**, *18*, 379.

(7) de Gennes, P.-G. *Macromolecules* **1976**, *9*, 587, 594.
(8) de Gennes, P.-G. "Scaling Concepts in Polymer Physics"; Cornell University Press: London, 1979.
(9) Brochard, F.; de Gennes, P.-G. *Macromolecules* **1977**, *10*, 1157.
(10) Brochard, F. *J. Phys. (Les Ulis, Fr.)* **1983**, *44*, 39.
(11) Chu, B.; *Polym. J. (Tokyo)* **1985**, *17*, 225.
(12) Koberstein, J. T.; Picot, C.; Benoit, H. *Polymer* **1985**, *26*, 673.
(13) Eisele, M.; Burchard, W. *Macromolecules* **1984**, *17*, 1636.
(14) Provencher, S. W.; Hendrix, J.; De Maeyer, L.; Paulussen, N. *J. Chem. Phys.* **1978**, *69*, 4273.
(15) Provencher, S. W. *Makromol. Chem.* **1979**, *180*, 201.
(16) Nishio, I.; Wada A. *Polym. J. (Tokyo)* **1980**, *12*, 145.
(17) Hwang, D.-h.; Cohen, C. **Macromolecules** **1984**, *17*, 1679; **1984**, *17*, 2890.
(18) Mathiez, P.; Mouttet, C.; Weisbuch, G. *J. Phys. (Les Ulis, Fr.)* **1980**, *41*, 519.
(19) Brown, W. *Macromolecules* **1985**, *18*, 1713.
(20) Brown, W. *Macromolecules*, in press.
(21) Brown, W. *Macromolecules* **1984**, *17*, 66.
(22) Amis, E.; Han, C. C. *Polymer* **1982**, *23*, 1047.
(23) Amis, E.; Han, C. C.; Matsushita, Y. *Polymer* **1984**, *25*, 650.
(24) Balloge, S.; Tirrell, M. *Macromolecules* **1985**, *18*, 817.
(25) Adam, M.; Delsanti, M. *Macromolecules* **1977**, *10*, 1229.
(26) Munch, J. P.; Herz, J.; Boileau, S.; Candau, S. *Macromolecules* **1981**, *14*, 1370.
(27) Schaefer, D. W.; Joanny, J. F.; Pincus, P. *Macromolecules* **1980**, *13*, 1280.
(28) Nemoto, N.; Makita, Y.; Tsunashima, Y.; Kurata, M. *Macromolecules* **1984**, *17*, 2629.
(29) Johnsen, R. M. *Proc. 27th Microsymp. Macromol.* **1984**.
(30) Zimmermann, K.; Delaye, M.; Licinio, P. *J. Chem. Phys.*, in press.
(31) Claesson, S. *Nature (London)* **1946**, *158*, 834.
(32) Roots, J.; Nyström, B. *Macromolecules* **1980**, *13*, 1595.
(33) Geissler, E.; Hecht, A. M. *J. Phys. Lett.* **1979**, *40*, L-173.
(34) Schaefer, D. W.; Han, C. C. In "Dynamic Light Scattering"; Pecora, R., Ed.; Plenum: New York, 1985.
(35) Saeki, S.; Konno, S.; Kuwahara, N.; Nakata, M.; Kaneko, M. *Macromolecules* **1974**, *7*, 521.
(36) Wiltzius, P.; Haller, H. R.; Cannell, D. S.; Schaefer, D. W. *Phys. Rev. Lett.* **1983**, *51*, 1183.
(37) Amirzadeh, J.; McDonnell, M. E. *Macromolecules* **1982**, *15*, 927.
(38) Adam, M.; Delsanti, M. *J. Phys. (Les Ulis, Fr.)* **1980**, *41*, 713.
(39) Wiltzius, P.; Haller, H. R.; Cannell, D. S.; Schaefer, D. W. *Phys. Rev. Lett.* **1984**, *53* (8), 834.
(40) Muthukumar, M.; Edwards, S. F. *Polymer* **1982**, *23*, 345.
(41) Callaghan, P. T.; Pinder, D. N. *Macromolecules* **1984**, *17*, 431.
(42) Candau, S. J.; Butler, I.; King, T. A. *Polymer* **1983**, *24*, 1601.
(43) Ewen, B.; Richter, D.; Hayter, J. B.; Lehnen, B. *J. Polym. Sci., Polym. Lett. Ed.* **1982**, *20*, 233.
(44) Radii of gyration, R_g, in the good solvent THF were assumed to approximate those in benzene for which a relationship between R_g and M is given in ref. 25. R_g values in cyclopentane were assumed to equal those in cyclohexane, from the relationship in ref 38. R_g values in ethyl acetate are obtained by assuming equality with dimensions in another marginal solvent, di-*n*-butyl phthalate.[42] The R_g values lay in the ratio 1:0.85:0.44. These R_g data were used to estimate approximate overlap concentrations from $C^* = 3M/\pi R_g^3 N_A$.

Monte Carlo Simulation of the Formation of Irregular Structures in Poly(vinyl chloride)

Alain Guyot

C.N.R.S.—Laboratoire des Matériaux Organiques, BP 24, 69390 Lyon Vernaison, France.
Received July 15, 1985

ABSTRACT: The Monte Carlo simulation of the formation of structural defects is carried out with microcomputers programmed in Basic. It is based on the most recent data for the polymerization mechanism and allows an interpretation of structural defects before and after the pressure drop. The deficiency in our knowledge of the mechanisms is pointed out, and some suggestions to fill the gap are discussed.

Introduction

The mechanism of the thermal degradation of poly(vinyl chloride) (PVC) is not yet fully clarified;[1-3] however, because it was shown in early work that the model compounds for the regular structures of PVC, such as the various isomers of 2,4-dichloropentane and 2,4,6-trichloroheptane, are thermally stable at the processing temperature, it is generally believed that the irregular structures—especially allylic and tertiary chlorides—are related to the initiation of the unzippering dehydrochlorination process. Consequently, the physicochemical analysis of these defects and the mechanism of their generation have been research objectives for a long time. Following the use of sophisticated NMR methods[4-6] as well as the formation of a 5 year cooperative IUPAC working party devoted to that subject,[7,8] major progress has been achieved recently for the first objective, although quantitative agreement between the results of ^{1}H NMR[8] and ^{13}C NMR[5] on the same samples is not totally satisfactory. On the other hand, assessing the importance of the head-to-head propagation mechanism, followed by isomerization and possible decomposition of the resulting radical, gave the key for understanding the main-chain end formation. In addition, most of the branching mechanisms that involve the transfer of the growing radical onto the polymer are also now understood. It then becomes possible, by assuming quantitative probabilities for the various products of these two basic mechanisms, to simulate the generation of the polymer molecules with their structural defects and chain ends.

Basic Features of the Simulation

The defects involved here are the chain ends, the branches and their associated branch points and ends, and the unsaturated structures, both at the chain ends and along the polymer backbone. The oxygenated structures coming from the byproducts of the reactions of accidental traces of oxygen are not considered here.

As for the chain ends, it has long been considered that, in addition to the radical-generated residues, they are produced by a transfer mechanism to the monomer; the transfer constant to the monomer is very large, 1.1×10^{-3} at 50 °C,[9] 10 times larger than the value expected for the reactivity of the poly(vinyl chloride) radical—which is similar to that of the poly(vinyl acetate) radical—or of the monomer structure, which might be compared to that of acrylonitrile. The corresponding transfer constants to the monomer are 2×10^{-4} for vinyl acetate and 1.7×10^{-5}[10] for acrylonitrile. The expected structures resulting from the possible mechanism of monomer transfer are shown in Scheme I. None of the unsaturated chain ends expected from this scheme have actually been observed with

0024-9297/86/2219-1090$01.50/0